

Neutrino induced reactions related to the ν -process nucleosynthesis of ^{92}Nb and ^{98}Tc

Myung-Ki Cheoun¹⁾ *, Eunja Ha¹⁾, T. Hayakawa²⁾, Satoshi Chiba²⁾, Ko Nakamura³⁾ Toshitaka Kajino^{3,4)}, Grant J. Mathews⁵⁾

1)Department of Physics, Soongsil University, Seoul 156-743, Korea

*2)Advanced Science Research Center, Japan Atomic Energy Agency,
2-4 Shirakata-shirane, Tokai, Ibaraki 319-1195, Japan*

3)National Astronomical Observatory, Mitaka, Tokyo 181-8589, Japan

*4)Department of Astronomy, Graduate School of Science,
University of Tokyo, 7-3-1 Hongo, Tokyo 113-0033, Japan*

*5)Center for Astrophysics, Department of Physics,
University of Notre Dame, IN 46556, USA*

(Dated: November 6, 2018)

Abstract

It has recently been proposed that $^{92}_{41}\text{Nb}$ and $^{98}_{43}\text{Tc}$ may have been formed in the ν -process. We investigate the neutrino induced reactions related to the ν -process origin of the two odd-odd nuclei. The main neutrino reactions for $^{92}_{41}\text{Nb}$ are the charged-current (CC) $^{92}\text{Zr}(\nu_e, e^-)^{92}\text{Nb}$ and the neutral-current (NC) $^{93}\text{Nb}(\nu(\bar{\nu}), \nu'(\bar{\nu})' n)^{92}\text{Nb}$ reactions. The main reactions for $^{98}_{43}\text{Tc}$, are the CC reaction $^{98}\text{Mo}(\nu_e, e^-)^{98}\text{Tc}$ and the NC reaction $^{99}\text{Ru}(\nu(\bar{\nu}), \nu'(\bar{\nu})' p)^{98}\text{Tc}$. Our calculations are carried out using the quasi-particle random phase approximation. Numerical results are presented for the energy and temperature dependent cross sections. Since charge exchange reactions by neutrons may also lead to the formation of $^{92}_{41}\text{Nb}$ and $^{98}_{43}\text{Tc}$, we discuss the feasibility of the $^{92}\text{Mo}(n,p)^{92}\text{Nb}$ and $^{98}\text{Ru}(n,p)^{98}\text{Tc}$ reactions to produce these nuclei.

PACS numbers: 25.30.Pt, 25.40.Kv, 26.30.-k, 26.30.Jk, 26.50.+x, 97.10.Cv

* Corresponding author : cheoun@ssu.ac.kr

I. INTRODUCTION

The neutrino (ν) process involves ν -induced reactions on various nuclei during core collapse supernovae (SN). This process has been proposed as the origin of some rare isotopes of light and heavy elements [1]. The cosmic abundances of these nuclei could thus be valuable tools for studying neutrino spectra from supernovae (SNe) [2, 3], and for constraining neutrino oscillation and/or other ν -physics parameters [4].

Among the many heavy elements, only the two isotopes ^{138}La and ^{180}Ta are currently thought to be synthesized primarily by the ν process [1, 2]. These two isotopes have similar features: they cannot be produced by either β^+ , EC, or β^- decays since in either case stable isobars shield against these decays. Not surprisingly then, the isotopic abundance ratios, $^{138}\text{La}/^{139}\text{La}$ and $^{180}\text{Ta}/^{181}\text{Ta}$, are quite small, *i.e.* 0.0902% and 0.012%, respectively [5], making them Nature's rarest isotopes.

In principle, any nuclide can be synthesized by the ν process in SN explosions. The produced abundances, however, are usually negligibly small because of the relevant reactions are mediated by a weak interaction compared to production via strong or electromagnetic interactions for the other major nucleosynthesis processes such as the s -, r -, and γ -processes. Thus, the ν process can only play a dominant role in the case of very rare isotopes that cannot be produced by other means. In the ν process, a nucleus can be synthesized by either a charged current (CC) or a neutral current (NC) reaction. Previous studies have concluded that contributions from the CC reactions are generally larger than those of the NC reactions for heavy nuclei [2, 6–8].

In a recent work [9], it has been pointed out that the nuclear chart around ^{92}Nb and ^{98}Tc is quite similar to that of ^{138}La and ^{180}Ta as shown in Figs. 1 and 2. Although both nuclei are unstable, their half-lives, 3.47×10^7 yr for ^{92}Nb and 4.2×10^6 yr for ^{98}Tc , are long enough to be observed on stellar surfaces or to be incorporated into meteorites. Moreover, they are shielded from β^+ , EC, or β^- decays because of the presence of neighboring stable isobars [10–14].

The isotopic abundance ratio of $^{92}\text{Nb}/^{93}\text{Nb}$ is known to be $\sim 10^{-3} - 10^{-5}$ at the time of solar system formation [15, 16]. This is comparable to the isotopic ratios for $^{138}\text{La}/^{139}\text{La}$ and $^{180}\text{Ta}/^{181}\text{Ta}$. Therefore, it has been proposed [9] that the two nuclei ^{92}Nb and ^{98}Tc may have a ν -process origin.

The main ν -process reactions for ^{92}Nb are the $^{92}\text{Zr}(\nu_e, e^-)^{92}\text{Nb}$ CC reaction and the $^{93}\text{Nb}(\nu(\bar{\nu}), \nu'(\bar{\nu}') n)^{92}\text{Nb}$ NC reaction, whereby neutrino-induced neutron emission to ^{92}Nb is followed by a NC neutrino reaction. For ^{98}Tc , the CC reaction, $^{98}\text{Mo}(\nu_e, e^-)^{98}\text{Tc}$, and the NC reaction, $^{99}\text{Ru}(\nu(\bar{\nu}), \nu'(\bar{\nu}') p)^{98}\text{Tc}$, with neutrino-induced proton emission to ^{98}Tc are believed to be the main reactions. Another NC reaction, $^{99}\text{Tc}(\nu(\bar{\nu}), \nu'(\bar{\nu}') n)^{98}\text{Tc}$, might also be possible because ^{99}Mo can easily β decay to ^{99}Tc . However, the half life of ^{98}Tc is 4.2×10^6 yr. This is longer than that of ^{99}Tc , 2.11×10^5 yr, so that ^{98}Tc may be difficult to produce by this NC reaction.

Moreover, if ^{98}Tc is produced by ν -induced reactions, it might β decay to $^{98}\text{Ru}^*$ which subsequently decays to its ground state with the emission of 0.74536 and 0.65243 MeV γ rays by E2 transitions. This situation closely resembles ^{26}Al , whose life time is 7.4×10^7 yr and decays to ^{26}Mg with a 1.809 γ ray (E2 transition) as observed by the COMPTEL detector on the Compton Gamma-Ray Observatory (CGRO) [17].

We presume a two step process in the ν -induced reaction: the 1st step is the formation of excited nuclei by incident ν 's; and the 2nd is the decay process to other ground states with some particle emission. To describe the 2nd decay process, one needs to consider the branching ratios for the decay processes by using a Hauser-Feshbach (HF) statistical model [18–22]. One also needs calculations of the transmission coefficients for the emitted particles. In this work, we made this calculation using the method of Refs. [18, 20].

The nuclear structure of ^{92}Nb and ^{98}Tc are key ingredients for this calculation. For example, the excited states with low spins in ^{92}Nb are strongly populated by a Gamow-Teller (GT) transitions from the 0^+ ground state of the ^{92}Zr seed nucleus. Our scheme for describing such excited states makes use of the standard quasi-particle random phase approximation (QRPA). For the NC reaction, $^{93}\text{Nb}(\nu, \nu')^{93}\text{Nb}$ and $^{99}\text{Ru}(\nu, \nu')^{99}\text{Ru}$, we generate the ground and excited states of the odd-even target nuclei, ^{93}Nb and ^{99}Ru , by applying a one quasi-particle operator to the even-even nuclei, ^{92}Zr and ^{98}Ru , which are assumed to be in the BCS ground state.

In Sec. II, we address a brief summary of our QRPA framework used in ν -induced reactions. In Sec. III, numerical cross sections for neutrino induced reactions on relevant nuclei are given in terms of the incident neutrino energy. Their temperature dependence is also presented for astrophysical applications under the assumption of a Fermi Dirac distribution for the SN neutrinos. A discussion about the roles of charge exchange reactions by neutron

capture on nuclei is also added to the results. A summary and conclusions are presented in Sec. IV.

II. THEORETICAL FRAMEWORK

Our QRPA formalism for the $\nu(\bar{\nu})$ -nucleus ($\nu(\bar{\nu}) - A$) reaction has been detailed in our previous papers [6–8]. Results from the QRPA have successfully described relevant ν -induced reaction data for ^{12}C , ^{56}Fe , ^{56}Ni , ^{138}La and ^{180}Ta as well as β , $2\nu 2\beta$ and $0\nu 2\beta$ decays. In particular, double beta (2β) decay is well known to be sensitive to the nuclear structure and has more data than the ν -induced reaction data. Therefore, it could be a useful tool for the estimation of ν -process reaction rates.

Charge exchange reactions, $A(n,p)B$ or $B(p,n)A$, also provide viable tests of nuclear models and one can deduce the neutrino induced reaction rates from these reactions because Gamow Teller (GT) transitions account for most of the strength in both the nucleon exchange reaction and the neutrino reactions, particularly in the low energy region.

Here we summarize two important characteristics regarding our calculation compared to other QRPA approaches. First, we utilize the Brueckner G matrix for the two-body interactions inside nuclei by solving the Bethe-Salpeter equation based on the Bonn CD potential for the nucleon-nucleon interactions in free space. This procedure reduces some of the ambiguities regarding nucleon-nucleon interactions inside nuclei.

Secondly, we include neutron-proton (np) pairing as well as neutron-neutron (nn) and proton-proton (pp) pairing correlations. Consequently, both CC and NC reactions can be described within a single framework.

The contribution from np pairing, however, has been shown to be only of order 1 ~ 2 % for the weak interaction on ^{12}C , such as β^\pm decay and the $\nu-^{12}\text{C}$ reaction [6, 7]. Such a small effect is easily understood because the energy gaps between the neutron and proton energy spaces in light nuclei are too large to be effective. However, in medium-heavy nuclei, such as ^{56}Fe and ^{56}Ni , the np pairing effect accounts for 20 ~ 30 % of the total cross section [7]. Therefore, in the heavy nuclei considered in this work, np pairing should be included.

The np pairing has two isospin contributions, $T = 1$ and $T = 0$. These correspond to $J = 0$ and $J = 1$ pairings, respectively. Since the $J = 0$ ($T = 1$) pairing couples a state to its time reversed state, the shape is almost spherical. Hence, the $J = 0$ ($T = 1$) np pairing can

be easily included in a spherical symmetric model.

The $J = 1$ ($T = 0$) np pairing, which is partly associated with the tensor force, however, leads to a non-spherical shape, *i.e.* deformation. Therefore, in principle, the $J = 1$ ($T = 0$) np coupling cannot be included in a spherically symmetrically model. However, if we use a renormalized strength constant for the np pairing, g_{np} , as a parameter to be fitted to the empirical pairing gaps, the $J = 1$ ($T = 0$) pairing can be incorporated implicitly even in a spherical symmetric model because the fitted g_{np} may include effectively the deformation of the nucleus.

The empirical np pairing gap is easily extracted from data on mass-excesses. The theoretical pairing gap $\delta_{np}^{th.}$ is calculated as the difference between the total energies with and without np pairing correlations [23]

$$\delta_{np}^{th.} = -[(H'_0 + E'_1 + E'_2) - (H_0 + E_1 + E_2)], \quad (1)$$

where $H'_0(H_0)$ is the Hartree-Fock energy of the ground state with (without) np pairing and $E'_1 + E'_2(E_1 + E_2)$ is the sum of the lowest two quasi-particles energies with (without) np pairing correlations. More detailed discussion of this is given at Ref. [23].

In our QRPA calculation, the ground state of a target nucleus is described by the BCS vacuum for the quasi-particle which comprises nn, pp and np pairing correlations. Excited states, $|m; J^\pi M\rangle$, in the compound nucleus are generated by operating the following one phonon operator on the initial BCS state

$$Q_{JM}^{+,m} = \sum_{kl\mu'\nu'} [X_{(k\mu' l\nu' J)}^m C^+(k\mu' l\nu' JM) - Y_{(k\mu' l\nu' J)}^m \tilde{C}(k\mu' l\nu' JM)] , \quad (2)$$

where the pair creation and annihilation operators, C^+ and \tilde{C} , are defined as

$$C^+(k\mu' l\nu' JM) = \sum_{m_k m_l} C_{j_k m_k j_l m_l}^{JM} a_{l\nu'}^+ a_{k\mu'}^+ , \quad \tilde{C}(k\mu' l\nu' JM) = (-)^{J-M} C(k\mu' l\nu' J - M) , \quad (3)$$

where $a_{\nu'}^+$ is a quasi-particle creation operator, and the $C_{j_k m_k j_l m_l}^{JM}$ are Clebsh-Gordan coefficients. Here Roman letters indicate single particle states, while Greek letters with a prime mean quasi-particle types 1 or 2.

If the neutron-proton pairing is neglected, quasi-particles become quasi-protons and quasi-neutrons, and the phonon operator is easily decoupled into two different phonon operators. One is for charge changing reactions such as nuclear β decay and CC neutrino

reactions. The other is for charge conserving reactions such as electromagnetic and NC neutrino reactions. The amplitudes $X_{a\alpha',b\beta'}$ and $Y_{a\alpha',b\beta'}$, which stand for forward and backward going amplitudes from the ground states to excited states, are obtained from the QRPA equation. A detailed derivation for this procedure was given in Refs. [7, 23]

By using the phonon operator $Q_{JM}^{+,m}$ in Eq.(2), we obtain the following expression for the CC neutrino reactions

$$\begin{aligned} & \langle QRPA || \hat{\mathcal{O}}_\lambda || \omega; JM \rangle \\ &= \sum_{a\alpha' b\beta'} [\mathcal{N}_{a\alpha' b\beta'} \langle a\alpha' || \hat{\mathcal{O}}_\lambda || b\beta' \rangle [u_{pa\alpha'} v_{nb\beta'} X_{a\alpha' b\beta'} + v_{pa\alpha'} u_{nb\beta'} Y_{a\alpha' b\beta'}] , \end{aligned} \quad (4)$$

where $\mathcal{N}_{a\alpha' b\beta'}(J) \equiv \sqrt{1 - \delta_{ab} \delta_{\alpha'\beta'} (-1)^{J+T} / (1 + \delta_{ab} \delta_{\alpha'\beta'})}$. This form is also easily reduced to the result produced in the pn QRPA when the np pairing correlations are not included [24]

$$\langle QRPA || \hat{\mathcal{O}}_\lambda || \omega; JM \rangle = \sum_{apbn} [\mathcal{N}_{apbn} \langle ap || \hat{\mathcal{O}}_\lambda || bn \rangle [u_{pa} v_{nb} X_{apbn} + v_{pa} u_{nb} Y_{apbn}] . \quad (5)$$

Since NC reactions for ^{93}Nb and ^{98}Tc occur in odd-even nuclei, we need to properly describe the ground state of odd-even nuclei. The standard QRPA treats the ground state of even-even nuclei as the BCS vacuum, so it is not easily applicable to reactions on odd-even nuclei.

Our formalism to deal with such NC reactions is based upon the quasi-particle shell model (QSM) [8]. First, we generate low energy spectra of odd-even nuclei by applying the one quasi-particle creation operator on the even-even nuclei constructed by the BCS theory, *i.e.* $|\Psi_i \rangle = a_{i\mu}^+ |BCS \rangle$ and $|\Psi_f \rangle = a_{f\nu}^+ |BCS \rangle$. Then the NC weak transitions are given by

$$\begin{aligned} & \sum_{i\mu' f\nu'} \langle J_f || \hat{\mathcal{O}}_\lambda || J_i \rangle \\ &= \sum_{\mu' f\nu'} [\langle fp || \hat{\mathcal{O}}_\lambda || ip \rangle u_{fp\nu'} u_{ip\mu'} + (-)^{j_a + j_b + \lambda} \langle ip || \hat{\mathcal{O}}_\lambda || fp \rangle v_{ip\mu'} v_{fp\nu'}] + (p \rightarrow n) . \end{aligned} \quad (6)$$

The weak current operator is comprised of longitudinal, Coulomb, electric and magnetic operators, $\hat{\mathcal{O}}_\lambda$, as described in Ref. [7]. Finally, with the initial and final nuclear states specified, the cross sections for $\nu(\bar{\nu}) - A$ reactions through the weak transition operator can be directly calculated by using the formulas of Refs. [25, 26]. For CC reactions we multiplied by the Cabbibo angle $\cos^2\theta_c$ and took account of the Coulomb distortion of the outgoing leptons [18, 24].

III. RESULTS AND DISCUSSIONS

Here we show results for ν -induced reactions for ^{92}Nb and ^{98}Tc . Detailed formulae for the cross sections were presented in our previous papers [7, 8]. For CC reactions, we consider Coulomb distortion of the outgoing lepton. Since the neutrino energies of interest here can go up to 80 MeV, we divide the energy range into two regions. In the low energy region, we use the Fermi correction used for the s-wave electron in β decay. In the high energy region, however, we exploit the effective momentum approach (EMA) used for higher energy electron scattering analysis [27, 28]. To make a smooth transition of the cross sections between the two energy limits, we determine an energy point, dubbed as the Coulomb cut, below which we use the Fermi correction and above which the EMA is used. We show results for two different Coulomb cuts, 30 and 40 MeV. Cases of 30 MeV change more smoothly. Fortunately, however, as we show here, the temperature dependent cross sections are nearly independent of the Coulomb cut.

Incident $\nu(\bar{\nu})$ energies emitted in SN explosions [1, 4] are assumed to be in the energy range from a few to tens of MeV because the $\nu(\bar{\nu})$ energy spectra emitted from the proto-neutron star are presumed to follow the Fermi-Dirac distribution given by a temperature T and chemical potential α [4, 34]. Therefore, the temperature dependence of the cross sections are averaged over the ν -distribution as follows

$$\langle \sigma_\nu \rangle = \int dE_\nu \sigma_\nu(E_\nu) f(E_\nu), \quad f(E_\nu) = \frac{E_\nu^2}{\exp[(E_\nu/T) - \alpha] + 1}, \quad (7)$$

where $\sigma_\nu(E_\nu)$ and $f(E_\nu)$ are the energy dependent ν - A cross sections and the corresponding neutrino flux, T and α can be chosen for a given neutrino type [4].

Since we are interested in the nuclear abundances of ^{92}Nb and ^{98}Tc , our temperature dependent cross sections are presented by multiplying the particle emission branching ratios by the cross sections for the formation of the compound nuclei. The branching ratios used here are based on the Hauser-Feshbach statistical model [19], using the JENDL3-3 model of Ref. [20] along with the calculated transmission coefficients.

A. Results for ^{98}Tc

Figure 3 shows the energy (upper) and temperature (lower panels) dependent cross sections for CC reactions on ^{98}Tc , *i.e.* $^{98}\text{Mo}(\nu_e, e^-)^{98}\text{Tc}$. In the upper panels, the case of a

30 MeV Coulomb cut seems to be smoother [24], so that it seems to be more reasonable than the 40 MeV case. The final total cross sections, however, are nearly indistinguishable. Our energy dependent cross sections show the typical behavior for CC cross sections for even-even nuclei. Namely, GT 1^+ and Fermi 0^+ transitions dominate the total cross section below 40 MeV. However, the contributions from higher multipole transitions, such as spin dipole resonance (SDR) contributions, increase above 40 MeV.

The red curves in the lower panels show the temperature dependent cross section for the CC reaction. Different Coulomb cuts do not affect cross sections, if we compare left and right low panels. Blue and green curves show cross sections multiplied by the branching ratios of the compound nuclei, ^{98}Tc , for proton and neutron decays. Since the neutron separation energy of ^{98}Tc , $S_n = 7.279$ MeV, is larger than the proton separation energy, $S_p = 6.176$ MeV, proton decay is much easier than neutron decay and leads to a larger cross section than that of the neutron decay. Of course, these two decays have no direct relationship to the formation of ^{98}Tc .

Figure 4 shows the results for the energy dependent cross sections for the NC reactions $^{99}\text{Ru}(\nu(\bar{\nu}), \nu'(\bar{\nu}'))^{99}\text{Ru}$, which have no Coulomb distortion. The upper two figures are for incident ν_μ (left) and ν_e (right). The lower two results are for their anti-neutrinos, *i.e.* $\bar{\nu}_\mu$ (left) and $\bar{\nu}_e$ (right). One can note that cross sections for ν_e and ν_μ are almost identical, but those by anti-neutrinos are different from those of incident neutrinos if we note differences between upper and lower panels. Therefore, the NC reactions are nearly independent of the neutrino species, but rather they depend on the helicity of the relevant neutrinos. It is an interesting point that the cross sections by incident ν are larger than those by incident $\bar{\nu}$ even in the case of NC reactions [35]. All cross sections below 40 MeV are dominated by the GT 1^+ transition, which is typical of NC reactions.

Figure 5 shows the temperature dependent cross sections corresponding to Fig.4, *i.e.* upper and lower two curves are for ν_μ (left) and ν_e (right), and $\bar{\nu}_\mu$ (left) and $\bar{\nu}_e$ (right), respectively. Here we have only shown results for a Coulomb cut = 40 MeV because they are nearly independent of the cuts as shown in Fig. 3. The red curves are for the cases of no decay, the blue and green curves include branching ratios for neutron and proton emission decays *i.e.* $^{99}\text{Ru}(\nu(\bar{\nu}), \nu'(\bar{\nu}')) n)^{98}\text{Ru}$ and $^{99}\text{Ru}(\nu(\bar{\nu}), \nu'(\bar{\nu}')) p)^{98}\text{Tc}$, respectively. Similarly to the energy dependent cross sections, they are independent of the neutrino species, but depend upon neutrino helicities as can be seen in Fig. 4. These results show that, in contrast

to the results by CC, the cross sections for proton emission decay are smaller than those for neutron emission decay because $S_n = 7.464$ MeV is smaller than $S_p = 8.478$ MeV in ^{99}Ru .

In particular, the green curves, $^{99}\text{Ru}(\nu(\bar{\nu}), \nu'(\bar{\nu}') p)^{98}\text{Tc}$, are important contributions to the formation of ^{98}Tc . This temperature dependence could play a vital role in understanding the neutrino temperatures at the astrophysical sites. Since in the formation of ^{98}Tc , the nucleus may have β decayed to ^{98}Ru with a half life of 4.2×10^6 yr and subsequently decayed to its ground state by E2 transitions by emitting 0.74536 MeV and 0.65243 MeV γ rays, which might be observable just like ^{26}Al in the Galaxy.

B. Results for ^{92}Nb

Here we show results for the neutrino induced reactions for ^{92}Nb , whose abundance and isotopic ratio $^{92}\text{Nb}/^{93}\text{Nb}$ are of astrophysical importance because they are thought to be produced by the ν process and can also be used as a cosmological chronometer [10].

The upper panels in Fig. 6 are the energy dependent cross sections for $^{92}\text{Zr}(\nu_e, e^-)^{92}\text{Nb}$. Likewise for the CC reaction for ^{98}Tc , the 30 MeV Coulomb cut is more reasonable for the Coulomb correction, but the location of the cut does not affect the temperature dependent cross sections as shown in the lower panels. Since the neutron separation energy of ^{92}Nb $S_n = 7.883$ MeV is larger than the proton separation energy $S_p = 5.846$ MeV, the proton decay is much easier than the neutron decay and leads to a larger cross section than that of neutron decay, similar to the case for ^{98}Tc .

All of the results for the ν -induced reactions on ^{98}Nb resemble those for ^{92}Tc . The strong energy and temperature dependence of the cross sections, in particular the red curves in the lower panels may give a clue to deduce the temperature conditions in the astrophysical sites producing ^{92}Nb . The results for ^{92}Nb for neutrino induced reactions via NC are presented in Fig.7, where only results for the ν_e and $\bar{\nu}_e$ are given because they are almost identical to those for the ν_μ and $\bar{\nu}_\mu$ reactions.

The general trends in the energy and temperature dependent cross sections by NC for ^{92}Nb are shown in Fig.8. They have no special characteristics compared to the results for ^{98}Tc in Fig. 5 except that the cross section for proton emission decay is larger than that for neutron emission decay because $S_n = 8.831$ MeV is larger than $S_p = 6.043$ MeV in ^{93}Nb . The magnitudes of the cross sections are about 1.5 times smaller than those for ^{98}Tc . This

reflects the fact that the cross sections for ν induced reactions are usually proportional to the masses of the target nuclei [7, 8].

C. Charge exchange reactions for ^{98}Tc and ^{92}Nb

We note here that the progenitor $15 M_{\odot}$ model of Heger and Woosley [29] shows significant ^{92}Nb presence before the supernova shock. Presumably this arises from the charge exchange reaction $^{92}\text{Mo}(n,p)^{92}\text{Nb}$ during core carbon burning. However, their network calculation does not take account of the (n, γ) destruction of ^{92}Nb which would happen. Therefore, we now discuss the feasibility of the formation of ^{98}Tc and ^{92}Nb nuclei by the (n,p) reactions, *i.e.* $^{98}\text{Ru}(n,p)^{98}\text{Tc}$ and $^{92}\text{Mo}(n,p)^{92}\text{Nb}$, in the s-process occurring in core helium burning during the pre-supernova evolution, and also the (n, γ) destruction of ^{92}Nb .

The Q value for the former is negative $Q_{np} = -1.014$ MeV, so that even neutrons with energies around a few hundred keV cannot be captured to produce ^{98}Tc . However, the $^{92}\text{Mo}(n,p)^{92}\text{Nb}$ reaction, whose Q value is $Q_{np} = 0.42671$ MeV, may occur for neutrons at $E \sim 30 - 100$ keV, if we consider the following discussion.

The J^{π} for states below ~ 0.5 MeV in ^{92}Nb are $J^{\pi} = 7^{+}(0.0)$, $2^{+}(0.135)$, $2^{-}(0.225)$, $3^{+}(0.285)$, $5^{+}(0.353)$, $3^{-}(0.390)$, $4^{+}(0.480)$ and $6^{+}(0.501)$. Therefore, two lowest states of the $^{92}\text{Nb} + p$ system are $J^{\pi} = \frac{15}{2}^{+}$ or $\frac{13}{2}^{+}$ for the ground and $J^{\pi} = \frac{5}{2}^{+}$ or $\frac{3}{2}^{+}$ for the 1st excited states. Since the initial system, $^{92}\text{Mo} + n$, is given as $0^{+} \otimes \frac{1}{2}^{+} \otimes l_n^{\pi}$, we need at least p-wave neutrons, *i.e.* $l_n^{\pi} \geq 1^{-}$.

Even if we consider the excited states of ^{92}Nb below ~ 0.5 MeV, which could be populated at a stellar temperature of $T_9 = T/10^9 K \approx 0.3$ for the s-process (*i.e.* typical neutron energy ~ 30 keV) because $E_n(= 30 \text{ keV}) + Q_{np}(= 0.43 \text{ MeV}) \simeq 0.5$ MeV, only the 2^{-} (0.225) and 3^{-} (0.389) states are allowed with $l_p^{\pi} = 1^{-}$ and 2^{+} protons by the conservation of relevant angular momenta.

We do not have any experimental data for the reaction $^{92}\text{Mo}(n,p)^{92}\text{Nb}$ below 1.5 MeV. According to theoretical calculations by ENDF/B-VII.0 [30], however, this reaction cross section might be lower than $0.1 \mu b$ for neutrons at energies below 1 MeV. Therefore the cross sections at about 30 keV neutrons might be much smaller than $0.1 \mu b$. We carried out a HF statistical model calculation at the threshold energy region as employing the JENDL-4 data [31]. The calculated Maxwellian-averaged cross sections for $^{92}\text{Mo}(n,p)^{92}\text{Nb}$ turn out to

be extremely small $\langle \sigma v \rangle / v_T = 4.02 \times 10^{-13} \mu b$ and $5.39 \times 10^{-4} \mu b$ at the neutron energies 30 keV and 100 keV, respectively, where $\langle \quad \rangle$ denotes an average with respect to the Maxwellian spectrum, σ is the cross section, v is the relative velocity of the neutrons and target nucleus, and v_T is the mean thermal velocity.

Once ^{92}Nb is produced by the (n,p) reaction from ^{92}Mo , it is exposed simultaneously to an intense flux of neutrons and destroyed by the radiative neutron capture reaction $^{92}\text{Nb}(n,\gamma)^{93}\text{Nb}$. Although the (n, γ) cross section was not measured for the radioactive nucleus ^{92}Nb ($\tau_{1/2} = 3.47 \times 10^7 y$), the $^{92}\text{Nb}(n,\gamma)^{93}\text{Nb}$ cross section is expected to be as large as those measured for stable Nb isotopes, $\langle \sigma v \rangle / v_T = 261.3$, 317.2, and 402.6 *mb* for $^{93,94,95}\text{Nb}(n,\gamma)^{94,95,96}\text{Nb}$ reactions, respectively, at the neutron energy 30 keV [20]. These (n, γ) cross sections are eighteen orders of magnitude larger than the $^{92}\text{Mo}(n,p)^{92}\text{Nb}$ cross section at this energy. Therefore, the $^{92}\text{Mo}(n,p)^{92}\text{Nb}$ reaction should not contribute much to the production of ^{92}Nb in the weak s-process in core helium burning phase of massive stars before explosion.

IV. SUMMARY

We have calculated neutrino induced reactions on two odd-odd nuclei, ^{98}Tc and ^{92}Nb by the Quasi-particle RPA method because both nuclei may be produced by the ν process in the explosive astrophysical objects. The abundance of ^{98}Tc can be measured by observing the γ -ray from the E2 transition to ^{98}Ru . Consequently, it may play a role as another γ -ray source for astrophysical observation similar to ^{26}Al .

The abundance ratio of $^{92}\text{Nb}/^{93}\text{Nb}$ has a meaningful implication. The ratio could determine the various roles of neutrino properties in explosive nucleosynthesis because it is very rare compared to that of ^{138}La and ^{180}Ta whose isotopic abundances place valuable physical constraints on the production site [5].

The energy and temperature dependent cross sections for ^{92}Nb , $^{92}\text{Zr}(\nu_e, e^-)^{92}\text{Nb}$ by charged current (CC) and $^{93}\text{Nb}(\nu, \nu' n)^{92}\text{Nb}$ by neutral current (NC) are presented. For ^{98}Tc , the CC reaction $^{98}\text{Mo}(\nu_e, e^-)^{98}\text{Tc}$ and the NC reaction $^{99}\text{Ru}(\nu, \nu' p)^{98}\text{Tc}$ have been estimated using the QRPA. Particle emission decays of the compound nuclei produced by the ν process make use of branching ratios calculated in the framework of the Hauser-Feshbach statistical approach with theoretical transmission coefficients.

Our deduced cross sections for these nuclei show features typical of neutrino induced reactions by NC and CC. CC reactions are dominated by GT transition below 40 MeV, but other multipole transitions become large above that energy. In the case of the NC reactions, the GT dominance becomes more significant in the low energy region. One more point of note regarding the NC reactions is that neutrino reactions are nearly independent of neutrino species, but depend on the neutrino helicity.

Finally, discussions of the charge exchange reaction by thermal neutrons for these nuclei remind us that the $^{92}\text{Mo}(n,p)^{92}\text{Nb}$ reaction might affect the initial abundance ratio of $^{92}\text{Nb}/^{93}\text{Nb}$ before the explosion, while $^{98}\text{Ru}(n,p)^{98}\text{Tc}$ may not because of the negative Q_{np} value. However, the (n,p) reaction is expected to be impotent for the production of pre-existing ^{92}Nb because the $^{92}\text{Nb}(n,\gamma)^{93}\text{Nb}$ reaction cross section is $\sim 10^{18}$ times larger than that of $^{92}\text{Nb}/^{93}\text{Nb}$ for neutrons of the energy ~ 30 keV and such ^{92}Nb is quickly destroyed. Nevertheless, more thorough calculations are necessary before further decisive conclusions about the roles of charge exchange reactions for ^{92}Nb can be made. Nucleosyntheses in SN explosions which consider these neutrino reactions are in progress including more realistic calculations of the charge exchange reactions.

Acknowledgments

This work was supported by the National Research Foundation of Korea (2011-0003188) and one of authors, Cheoun, was supported by the Soongsil University Research Fund. This work was also supported in part by Grants-in-Aid for Scientific Research of JSPS (20244035), and in part by U.S. Department of Energy under Nuclear Theory Grant DE-FG02-95-ER40934, and in part by Grants-in-Aid for JSPS Fellows (21.6817)

-
- [1] S. E. Woosley, D. H. Hartmann, R. D. Hoffmann, and W. C. Haxton, *Astrophys. J.* **356**, 272 (1990).
- [2] A. Heger, E. Kolbe, W.C. Haxton, K. Langanke, G. Martínez-Pinedo, S.E. Woosley, *Phys. Lett.* **B606**, 258 (2005).
- [3] T. Yoshida, T. Kajino, D-H. Hartmann, *Phys. Rev. Lett.* **94**, 231101 (2005).
- [4] T. Yoshida, T. Kajino, H. Yokomukura, K. Kimura, A. Takamura, D-H. Hartmann, *Astrophys. J.* **649**, 319 (2006).
- [5] T. Hayakawa, T. Kajino, S. Chiba, G. Mathews, *Phys. Rev. C* **81**, 052801(R) (2010).
- [6] Myung-Ki Cheoun, Eunja Ha, S. Y. Lee, W. So, K. S. Kim and T. Kajino, *Phys. Rev. C* **81**, 028501 (2010).
- [7] Myung-Ki Cheoun, Eunja Ha, K. S. Kim and T. Kajino, *J. of Phys.* **G 37**, 055101, (2010).
- [8] Myung-Ki Cheoun, Eunja Ha, T. Hayakawa, S. Chiba and T. Kajino, *Phys. Rev. C* **82**, 035504, (2010).
- [9] T. Hayakawa, *Proceedings of Australian ..* (2011).
- [10] Q. Z. Yin, *et al.*, *Astrophys. J.* **536**, L49-L53 (2000).
- [11] D. D. Calyton, *et al.*, *Astrophys. J.* **214**, 300-315, (1977).
- [12] C. Münker, *et al.*, *Science*, **289**, 1538-1542 (2000).
- [13] Q. Z. Yin, S. B. Jacobsen, *LPI*, 5208, (2002).
- [14] B. S. Meyer, *Nucl. Phys.* **A719**, 13-20 (2003).
- [15] M. Schönbachler, *et al.*, *Science* **295**, 1705-1708, (2002).
- [16] M. Schönbachler, *et al.*, *Geochimica et Cosmochimica Acta*, **69**, 775-785, (2005).
- [17] <http://heasarc.gsfc.nasa.gov/docs/cgro/index.html>
- [18] T. Suzuki, S. Chiba, T. Yoshida, T. Kajino, T. Otsuka, *Phys. Rev. C* **74**, 034307 (2006).
- [19] W. Hauser and H. Feshbach, *Phys. Rev.* **87**, 366 (1952).
- [20] T. Nakagawa, S. Chiba, T. Hayakawa, T. Kajino, *Atomic Data and Nuclear Data Table*, **91**, 77, (2005).
- [21] T. Yoshida, T. Suzuki, S. Chiba, T. Kajino, H. Yokomukura, K. Kimura, A. Takamura, H. Hartmann, *Astro. Phys. J.* **686**, 448 (2008).
- [22] T. Suzuki, M. Honma, K. Higashiyama, T. Yoshida, T. Kajino, T. Otsuka, H. Umeda, and K.

- Nomoto, Phys. Rev. C **79**, 061603(R) (2009).
- [23] M. K. Cheoun, A. Bobyk, Amand Faessler, F. Simcovic and G. Teneva, Nucl. Phys. **A561**, 74 (1993) ; Nucl. Phys. **A564**, 329 (1993); M. K. Cheoun, G. Teneva and Amand Faessler, Prog. Part. Nuc. Phys. **32**, 315 (1994) ; M. K. Cheoun, G. Teneva and Amand Faessler, Nucl. Phys. **A587**, 301 (1995).
- [24] N. Paar, D. Vretenar, T. Marketin, and P. Ring, Phys. Rev. C **77**, 024608 (2008).
- [25] T. W. Donnelly and W. C. Haxton, ATOMIC DATA AND NUCLEAR DATA **23**, 103 (1979).
- [26] J. D. Walecka, *Muon Physics*, edited by V. H. Hughes and C. S. Wu (Academic, New York, 1975), Vol II.
- [27] A. Bortrungo and G. Co', Eur. Phys. J. **A24 S1**, 109, (2005).
- [28] Giampaolo Co', Acta Physica Polonica **B 37**, 2235, (2006).
- [29] S. E. Woosley and A. Heger, Phys. Rept. **442**, 269 (2007).
- [30] M. B. Chadwick *et. al*, Nuclear Data Sheets **107**, 2931, (2006).
- [31] K. Shibata *et. al*, J. Nucl. Sci. Tech. **48**, 1 (2011).
- [32] Harper, C. L. Jr., Astrophys. J. 466, 437 (1996).
- [33] Busso, M., Gallino, R. and Wasserburg, G.J. 1999, ARA&A, 37, 239
- [34] E. Kolbe, K. Langanke, G Martinez-Pinedo and P. Vogel, J. Phys. G **29**, 2569 (2003).
- [35] Myung-Ki Cheoun, Eunja Ha and T. Kajino, Phys. Rev. C **83** 0888 (2011).

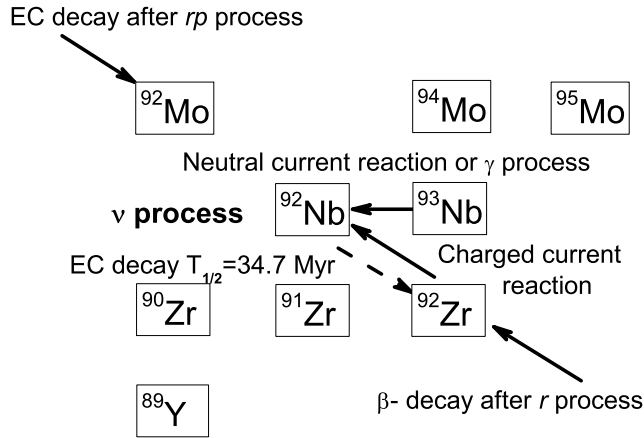


FIG. 1: Partial nuclear chart around ^{92}Nb and the main neutrino reactions, $^{92}\text{Zr}(\nu_e, e^-)^{92}\text{Nb}$ by charged current(CC) and $^{93}\text{Nb}(\nu(\bar{\nu}), \nu'(\bar{\nu})' n)^{92}\text{Nb}$ by neutral current(NC).

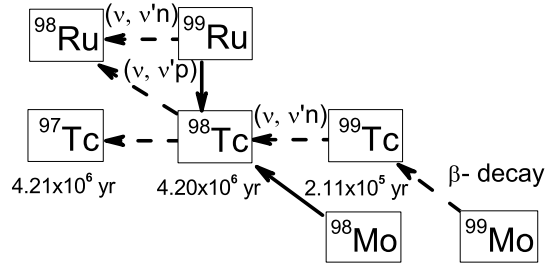


FIG. 2: Partial nuclear chart around ^{98}Tc and main neutrino reactions, $^{98}\text{Mo}(\nu_e, e^-)^{98}\text{Tc}$ by CC and $^{99}\text{Ru}(\nu(\bar{\nu}), \nu'(\bar{\nu})' p)^{98}\text{Tc}$ by NC.

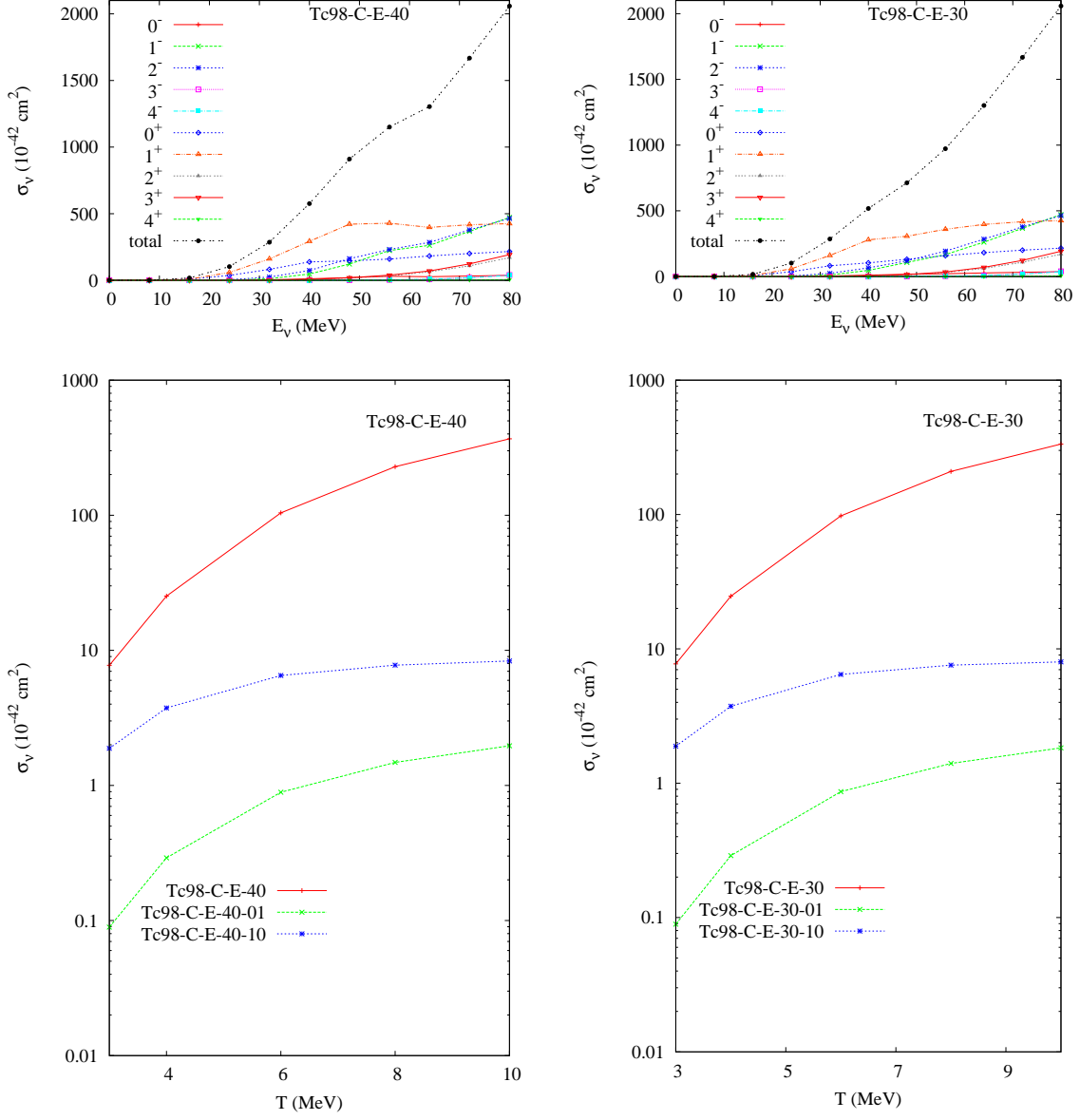


FIG. 3: Energy (upper) and temperature (lower) dependent cross sections of CC reaction for ^{98}Tc , $^{98}\text{Mo}(\nu_e, e^-)^{98}\text{Tc}$. The contribution of each multipole transition is also presented along with their sum. Left and right panels are for Coulomb cuts = 40 and 30 MeV (see text for more explanations), respectively. The red curves in the lower panels are cross sections for ^{98}Tc , $^{98}\text{Mo}(\nu_e, e^-)^{98}\text{Tc}$. Blue and green curves are for proton and neutron emission decays from $^{98}\text{Tc}^*$, *i.e.* $^{98}\text{Mo}(\nu_e, e^-p)^{97}\text{Mo}$ and $^{98}\text{Mo}(\nu_e, e^-n)^{97}\text{Tc}$.

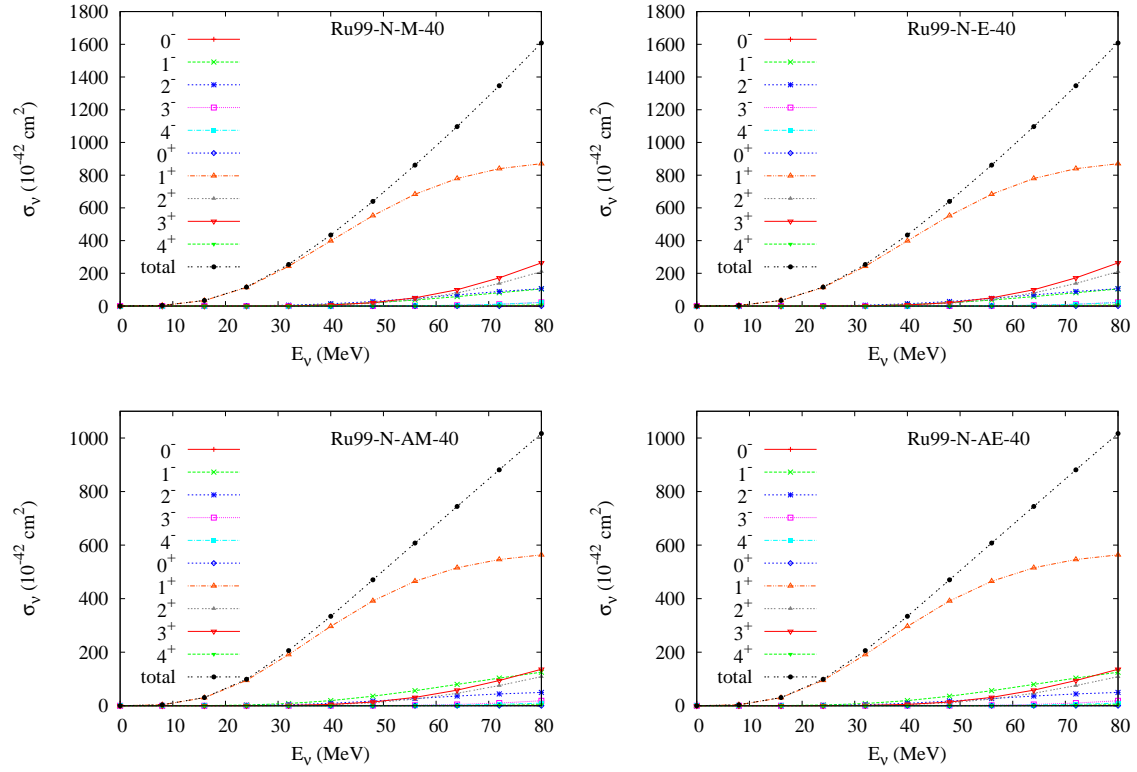


FIG. 4: Energy dependent cross sections of NC reactions for ^{98}Tc , $^{99}\text{Ru}(\nu(\bar{\nu}), \nu'(\bar{\nu}'))^{99}\text{Ru}$. The upper two figures are for incident ν_μ (left) and ν_e (right). The lower two results are for $\bar{\nu}_\mu$ (left) and $\bar{\nu}_e$ (right).

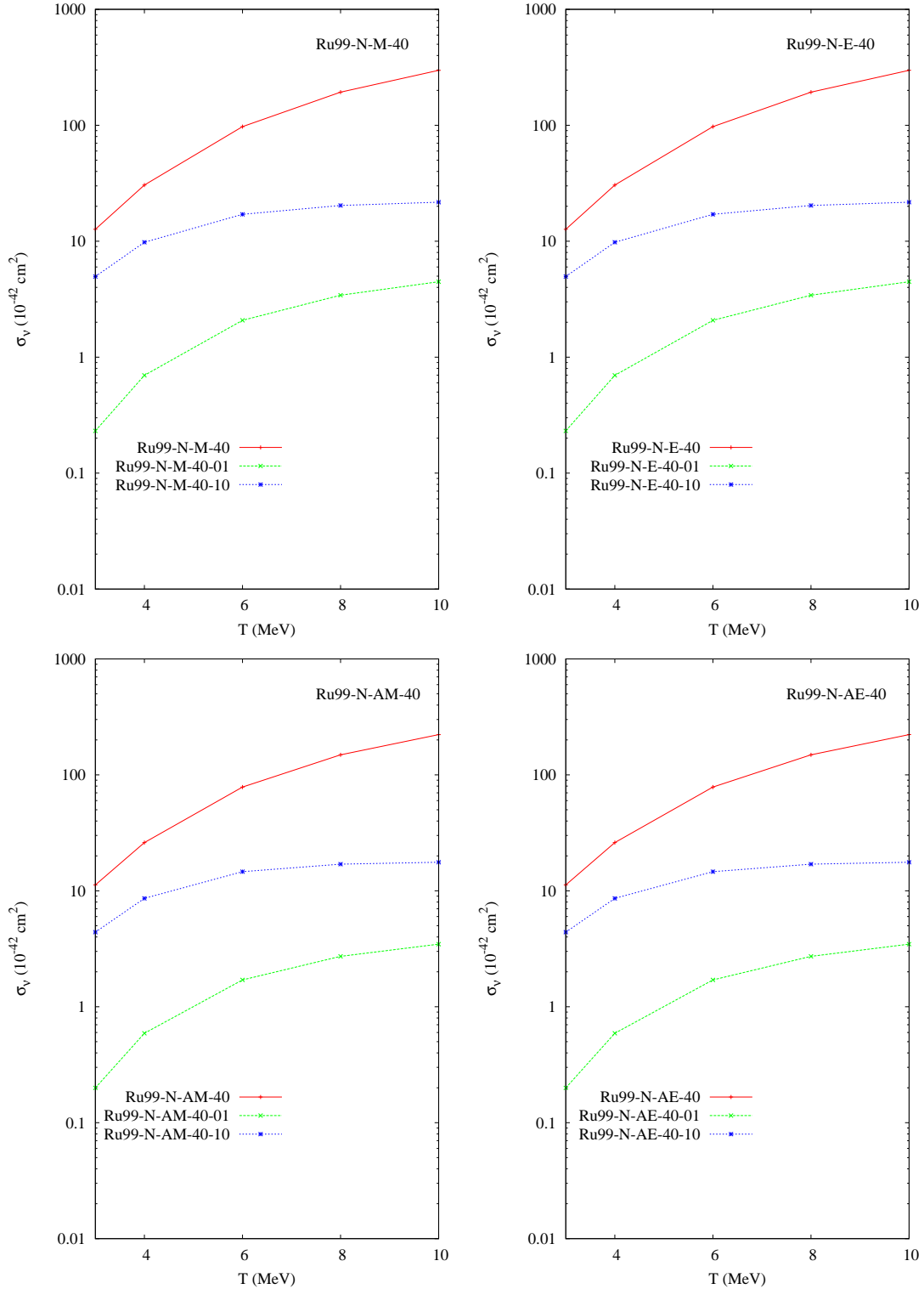


FIG. 5: Temperature dependent cross sections of NC reactions for ^{98}Tc . The upper two figures are for incident ν_μ (left) and ν_e (right). The lower two results are for $\bar{\nu}_\mu$ (left) and $\bar{\nu}_e$ (right). Red curves are $^{99}\text{Ru}(\nu(\bar{\nu}), \nu'(\bar{\nu}'))^{99}\text{Ru}$. Blue and green curves are for neutron and proton emission decays from $^{99}\text{Tc}^*$, *i.e.* $^{99}\text{Ru}(\nu(\bar{\nu}), \nu'(\bar{\nu}')n)^{98}\text{Ru}$ and $^{99}\text{Ru}(\nu(\bar{\nu}), \nu'(\bar{\nu}')p)^{98}\text{Tc}$.

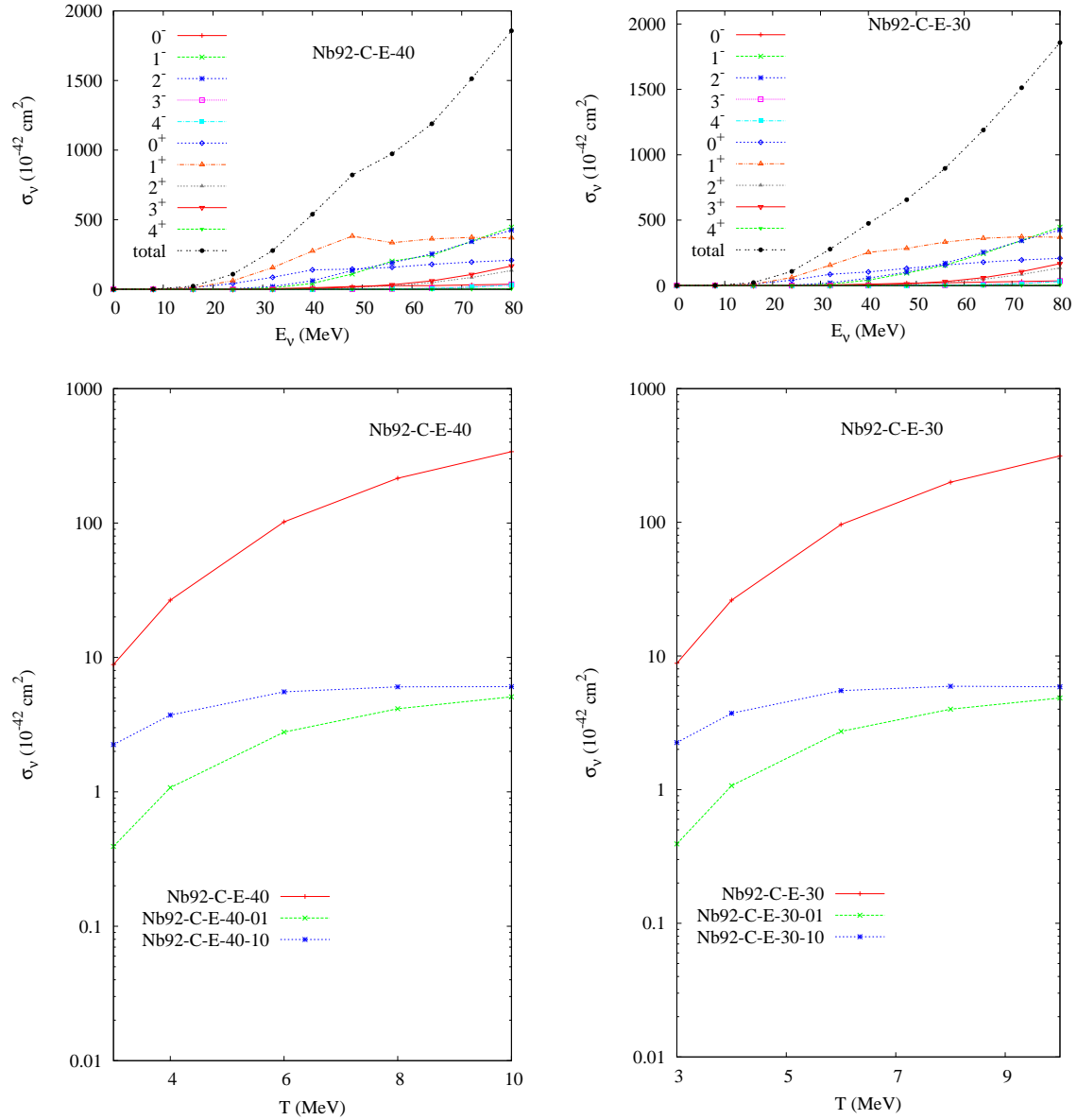


FIG. 6: Energy and temperature dependent cross sections of CC reactions for ^{92}Nb . Red curves in lower panels are cross sections for ^{92}Nb , $^{92}\text{Zr}(\nu_e, e^-)^{92}\text{Nb}$. Blue and green curves are for proton and neutron decays, *i.e.* $^{92}\text{Zr}(\nu_e, e^-p)^{91}\text{Zr}$ and $^{92}\text{Zr}(\nu_e, e^-n)^{91}\text{Nb}$.

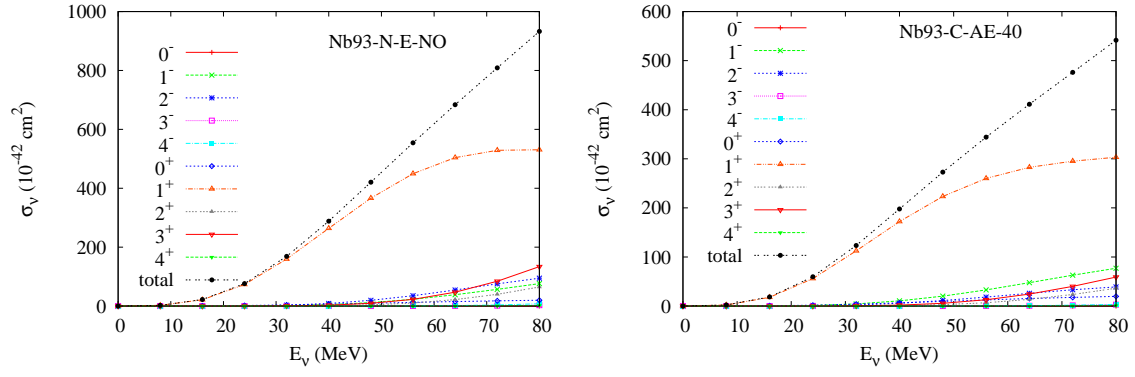


FIG. 7: Energy dependent cross sections of NC reactions for ^{92}Nb , $^{93}\text{Nb}(\nu(\bar{\nu}), \nu'(\bar{\nu}')n)^{93}\text{Nb}$. Left is for incident ν_e and right is for $\bar{\nu}_e$.

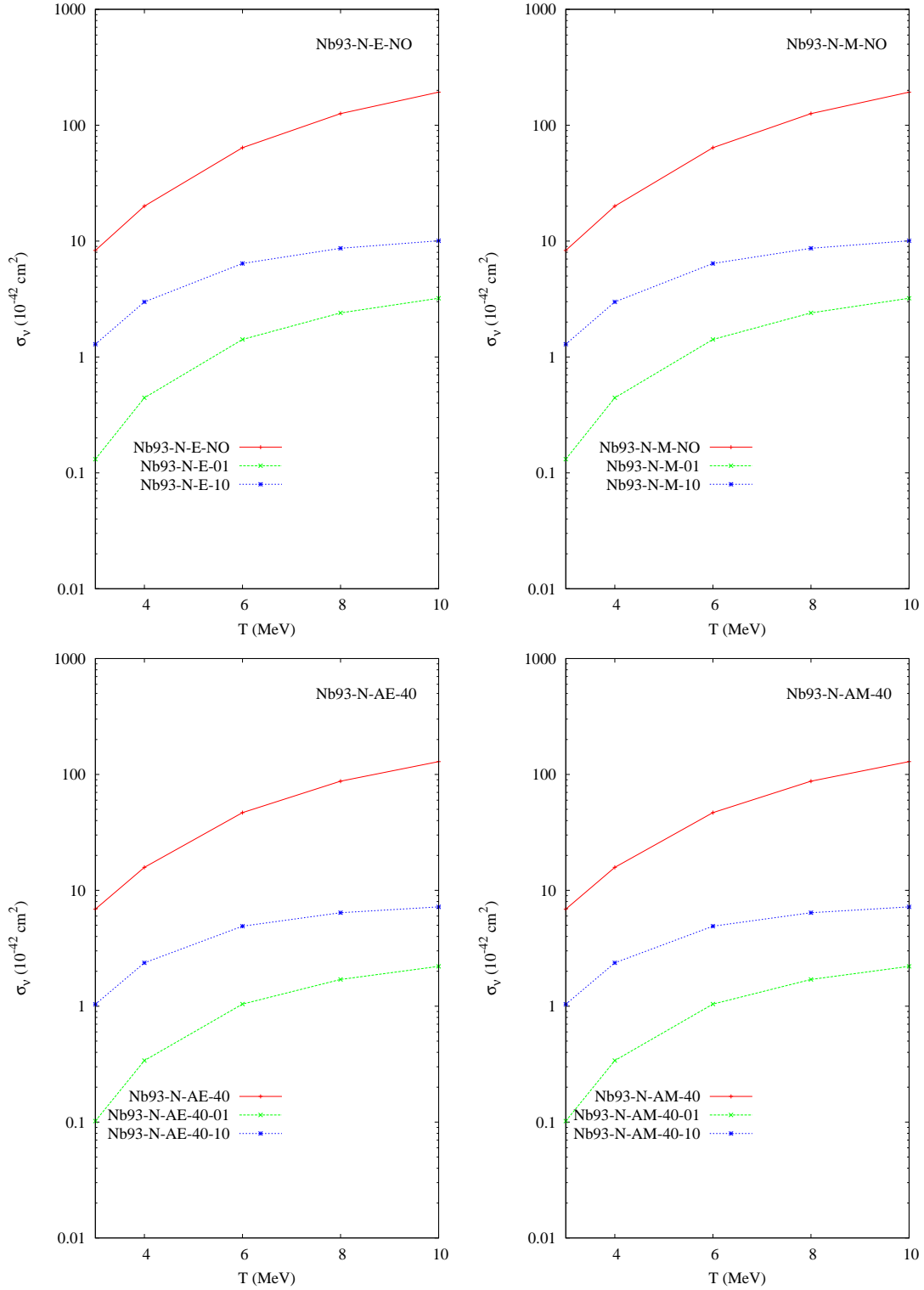


FIG. 8: Temperature dependent cross sections of NC reactions for ^{92}Nb . The upper two figures are for incident ν_e (left) and ν_μ (right). The lower two results are for $\bar{\nu}_e$ (left) and $\bar{\nu}_\mu$ (right). Red curves are $^{93}\text{Nb}(\nu(\bar{\nu}), \nu'(\bar{\nu}'))^{93}\text{Nb}$. Blue and green curves are for proton and neutron emission decays from ^{93}Nb , *i.e.* $^{93}\text{Nb}(\nu(\bar{\nu}), \nu'(\bar{\nu}'))p)^{92}\text{Zr}$ and $^{93}\text{Nb}(\nu(\bar{\nu}), \nu'(\bar{\nu}'))n)^{92}\text{Nb}$.